RECENT RESULTS FROM VERY HIGH ENERGY GAMMA RAY OBSERVATIONS IN THE NORTHERN HEMISPHERE

Frank Krennrich*
Iowa State University
Physics and Astronomy Department
Ames, IA 50011

ABSTRACT

The past decade has seen a major breakthrough in the field of Very High Energy (VHE) Gamma-Ray Astronomy at energies above 200 GeV. The TeV source catalog contains more than 6 active galactic nuclei, a nearby radio galaxy, supernova remnants, the detection of the first TeV unidentified source and a tentative detection of the Galactic Center. The recent success of VHE gamma-ray astronomy promises a broad range of astrophysical sources to be explored with next generation telescopes.

Astronomy with TeV photons is based on the ground-based detection of TeV gamma-rays using the imaging atmospheric Cherenkov technique. The charge of this talk is to describe the status of the field based on observations carried out in the Northern Hemisphere using atmospheric Cherenkov telescopes. For results from the Southern Hemisphere observatories see the paper by Tanimori in these conference proceedings.

*Supported by DoE High Energy Physics.

1 Introduction

The aim of VHE gammma-ray astronomy is to explore the non-thermal universe at the highest energies by the means of TeV photon beams. TeV gamma rays reveal direct information about the location of particle acceleration/interaction and gamma-ray emission sites. The production of TeV gamma rays in an astrophysical setting is closely linked to lower energy photons in the X-ray regime via synchrotron emission and inverse Compton scattering if the accelerated particles are electrons. Gamma-rays at the TeV scale can also be produced by the decay of neutral pions originating from hadronic interactions of cosmic rays with photon fields and atomic/neutral hydrogen.

Furthermore, scenarios based on particle physics theory and the desire for explaining the dark matter component of our universe suggest, that large density enhancements of supersymmetric particles may be detectable via annihilation and subsequent gamma-ray emission at tens of GeV to several hundred GeV (Ref. 78, Ref. 71). Another speculative possibility for gamma-ray emission considered is the evaporation of primordial black holes formed in the early universe (Ref. 33).

The scientific objective of observations of astrophysical TeV photons is to address a range of physics topics covering non-thermal astrophysics involving electrons and cosmic rays and particle astrophysics probing the universe for dark matter. TeV photon beams penetrating cosmological distances through extragalactic diffuse radiation fields and space, can also provide constraints for cosmology and potentially give some insights into fundamental physics such as quantum gravity.

In comparison to well developed disciplines in astrophysics it is important to note that TeV gamma-ray astronomy is a new field which is just starting to tap into the scientific potential of non-thermal emission from our Universe: less than 5% of the TeV sky has been explored at the sensitivity level of better than 100mCrab*.

The most sensitive technique to detect gamma rays from astrophysical sources is the imaging atmospheric Cherenkov technique (Ref. 80), pioneered by the Whipple collaboration. A VHE gamma ray when entering the earth's atmosphere initiates an electromagnetic air shower of secondary electrons/positrons emitting Cherenkov photons, which are beamed along the shower axis with an opening angle of less than a degree. This results in a light pool at the ground of 100 m to several hundred meters in diameter, depending on the primary particle's energy. Placing a large optical reflector

*In gamma-ray astronomy the flux sensitivity is generally expressed in units of the flux from the Crab Nebula which is a reference source also referred to as a standard candle.

within the lightpool allows the detection of the Cherenkov light. The size of the light pool determines the effective collection area which is typically 10^6 times larger than for a typical satellite-based gamma-ray detector ($0.1 - 1\mathrm{m}^2$).

By virtue of this intrinsically powerful technique TeV gamma-ray astronomy has matured over the last ten years to an astrophysical discipline capable of sampling gamma-ray lightcurves of variable sources and detecting flux changes as short as 30 minutes. Most relevant for the physics analysis of TeV gamma-ray sources is calorimetry of air showers: measurements of energy spectra between 250 GeV to 50 TeV are accurate enough to unravel spectral features such as cutoffs and curvature. The high sensitivity of the technique has led to some remarkable measurements and observations of gamma-ray emission from jets associated with the most massive black holes in the universe. These jets appear as some of the brightest objects in the universe when pointed towards the observer. Jets that originate in the proximity of a supermassive black hole located at the center of an active galaxy (often referred to as active galactic nuclei, AGN) provide a high energy window for studying processes near a black hole with masses of $10^6 - 10^9$ solar masses.

The current catalog of TeV gamma-ray sources contains a total of 18 sources, with 8 active galactic nuclei, a radio galaxy, a tentative detection of a starburst galaxy, 3 pulsar-powered nebulae, 6 shell-type supernova remnants (Ref. 39). I was asked to review recent results from observations by imaging atmospheric Cherenkov telescopes located in the northern hemisphere. The northern hemisphere sources are mostly extragalactic, hence the focus of this paper will be on observations and measurements of active galaxies. Also in addition the first unidentified TeV photon source is included in this review.

2 TeV Photons from Active Galaxies

Astronomers were taken by surprise when the discovery of the first extragalactic source of TeV gamma rays, Mrk 421 was announced in 1992 (Ref. 70). TeV gamma-ray emission from jets of active galaxies was not predicted by any AGN jet model (Ref. 17). The launch of the Compton Gamma Ray Observatory (CGRO) in 1991 and the discovery of GeV emission from radio loud galaxies by its EGRET detector fueled the expectations and prospects for detecting many more TeV gamma-ray emitting AGN. The most recent EGRET catalog (Ref. 31) contains more than 66 AGN, whereas to date the TeV catalog contains 8 AGN (Ref. 82). Most AGN detected at GeV and at TeV energies are classified as blazars (Ref. 6, Ref. 17), objects that contain a compact and flat spectrum radio source

and exhibit an optical non-thermal spectrum that is polarized and often highly variable. Most astronomers agree that blazars contain a jet with its axis closely aligned with the line-of-sight of the observer.

2.1 Compact Emission Regions in Blazars

Perhaps the most intriguing property of any gamma-ray emitting blazar observed to date is illustrated in Fig. 1, showing two lightcurves of Mrk 421 measured by the Whipple collaboration (Ref. 25).

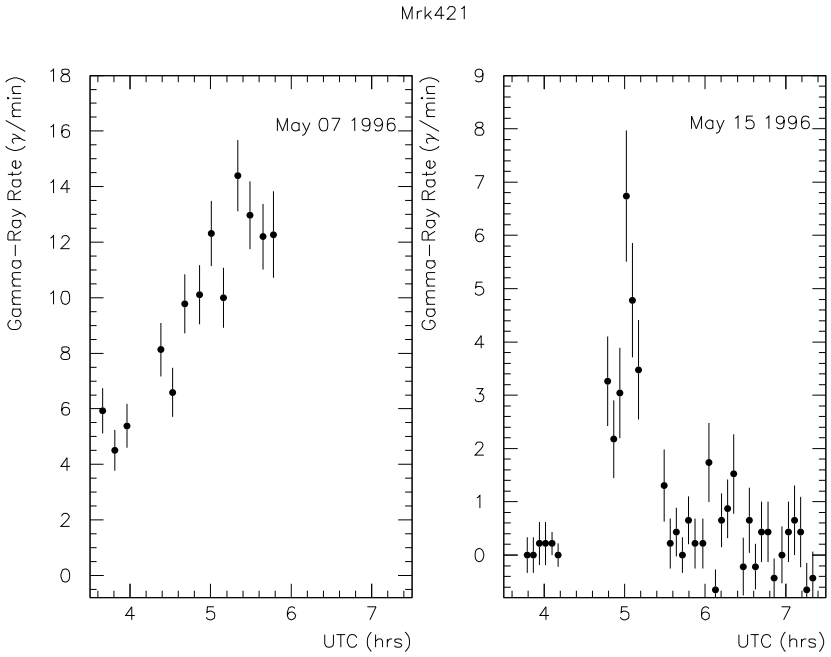

Fig. 1. The lightcurve for two gamma-ray flares from Mrk 421 on May 7 1996 and May 15 1996, the latter exhibiting the shortest variability time scale (15 minutes) observed of any gamma-ray observation at energies above 100 MeV (Ref. 25).

The short variability time scale of 15 minutes for the May 15 1996 lightcurve implies by causality that the emission region is constrained to a size of $10^{-4} - 10^{-5}$ pc or less (for details, see Ref. 25). The small emission region implies an extremely large energy density of VHE gamma rays in the emission region providing another important constraint: given a typical density of soft synchrotron photons (optical) in the jet and the high gamma-ray density, they should pair-produce with the latter and prevent gamma rays from escaping the emission region. A solution to this difficulty is to postulate relativistic boosting of the emission region towards the observer which reduces the

actual energy density in the comoving reference frame. Doppler factors[†] of $\delta = 5 - 10$ have been derived for the TeV emission regions in Mrk 421 and Mrk 501 (Ref. 25, Ref. 74, Ref. 13). AGN detected at TeV energies appear to have their jet axes closely aligned with the line of sight of the observer to a few degrees, supporting the picture that gamma-ray emitting AGN are blazars.

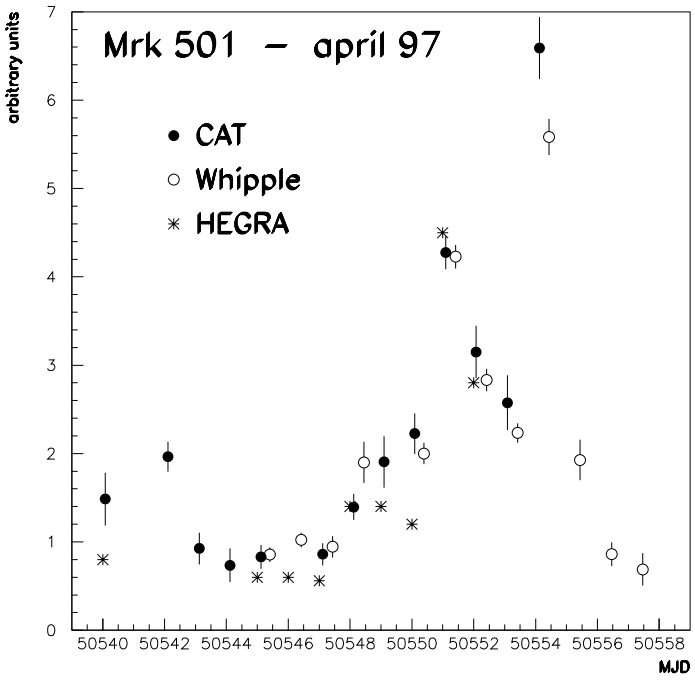

Fig. 2. This figure shows the lightcurve of Mrk 501 showing strong daily to weekly flux variations from an observing campaign in 1997 involving the CAT, HEGRA and the Whipple collaborations (Ref. 69).

Variability time scales of TeV blazars encompass hourly, daily, monthly to yearly time scales. A lightcurve from the combined results from several experiments (Ref. 69) with daily flux averages for the blazar Mrk 501 is shown in Fig. 2. Although the observations are offset in longitude, on average by 6 hours, the measurements of the daily averaged fluxes by the three experiments show a similar lightcurve.

Flaring activity of Mrk 501 on time scales of days to months and years is evident from Fig. 3.

Strong flares at TeV energies are a common feature of the known gamma-ray blazars. Another example is given in Fig. 4 showing the lightcurve for the blazar 1ES1959+650

[†]The Doppler factor δ is defined as $\delta^{-1} = \gamma(1 - \beta\cos\theta)$, where β and γ are the velocity and Lorentz factor of the emission region in the jet, and θ is the angle with respect to the observer.

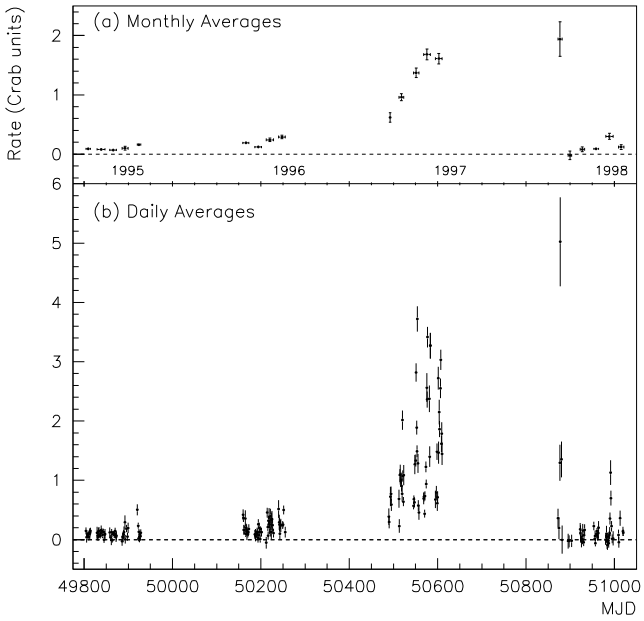

Fig. 3. a) shows the lightcurve for Mrk 501 between 1995 - 1998 including the episode of strong flaring activity in 1997 (Ref. 72) showing the monthly and yearly flux variations. b) shows the lightcurve for the same time period binned according to daily average, indicating daily flux variation on top of the monthly and yearly variations.

which was recently detected by several VHE groups. 1ES1959+650 was initially reported by the "Utah Seven Telescope Array" collaboration (Ref. 63) at the 3.9 sigma level, revived by a tentative detection by the the HEGRA collaboration in 2000 and 2001 (Ref. 43), confirmed in 2002 (Ref. 4) and finally established as a TeV source by a strong detection by the Whipple collaboration (Ref. 35).

Although lightcurves of VHE gamma-ray emission are invaluable for gaining a better understanding of the dynamics of the emission and acceleration processes at work, they are incomplete for testing basic jet emission models. The general picture which has emerged for the energy spectrum of non-thermal blazar emission includes two components: a low energy luminosity peak occurring in the radio/optical or X-rays and a high energy peak, falling somewhere between MeV to TeV energies. The low energy component with energies extended up to about 100 keV for the most extreme blazars, is universally attributed to synchrotron radiation from electrons. The high energy component with energies sometimes extending to the TeV range, is often attributed to inverse Compton scattering (Ref. 58, Ref. 60). The origin of the high energy component can also be explained by competing models (Ref. 55, Ref. 56, Ref. 57), which assume that it

arises from protons, either by proton-induced synchrotron cascades or by decays and/or interactions of secondary particles such as neutral pions and neutrons, or synchrotron radiation from proton beams (Ref. 62). A detailed discussion of blazar observations and relevant models can be found elsewhere (Ref. 17, Ref. 16).

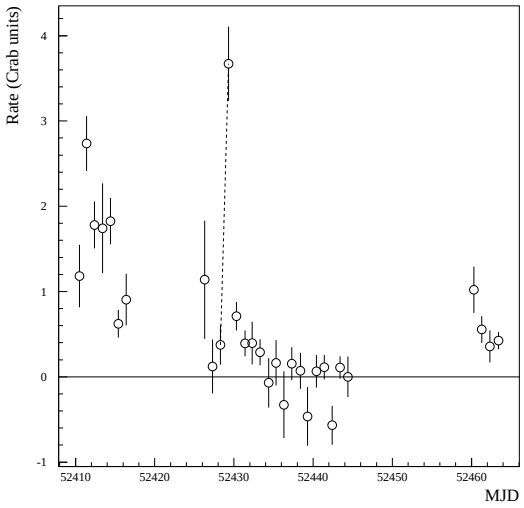

Fig. 4. The lightcurve for 1ES1959+650 showing a strong daily flux variation and also weekly variation (Ref. 35).

A very attractive and self-consistent model requiring the least number of adjustable parameters is the synchrotron-self Compton (SSC) model, in which energetic (typically TeV) electrons bound to a magnetic field emit synchrotron radiation and also boost some of these synchrotron photons via inverse Compton scattering to VHE gamma rays. The basic version of an SSC model is often referred to as one-zone SSC model in which a single emission region moving at relativistic speed along the jet axis is described. Testing such a model inevitably requires the observation of blazar flaring states over a wide range of energies, to cover the synchrotron emission and the inverse Compton component simultaneously. Relevant parameters are the Doppler factor, the maximum particle energy and the magnetic field strength in the jet. Such attempts to make multiwavelength observations are described in the next section.

2.2 Correlation between X-rays and TeV Photons

Non-thermal emission models that involve relativistic particles typically make predictions for a broad range of photon energies (radio - TeV gamma-ray); hence, multiwavelength observations are a key to the understanding of a specific TeV gamma-ray source. Observations of variable sources like blazars over a large range of time scales are difficult to coordinate when using a variety of instruments in space and at ground level. This is because the imaging atmospheric Cherenkov technique is limited to operation during dark moonless nights and pointed satellite instruments are difficult to allocate for a single target for extended periods of time. Therefore, multiwavelength campaigns provide sparse time coverage and generally have gaps for time scales beyond a few hours. Nevertheless, multiwavelength campaigns have furthered our understanding of VHE gamma-ray emission from blazar jets.

To illustrate the general connection between X-ray and TeV flaring activity we show in Fig. 5 the lightcurves of the six established TeV blazars (Ref. 44) from continuous monitoring at X-ray energies using the RXTE All-Sky Monitor (ASM). As can be seen in Fig. 5 the historical strong flaring state of Mrk 501 detected between early - late 1997 in TeV gamma rays (see also Fig. 3; Ref. 72, Ref. 69) has a counterpart in X-rays also showing a strong enhancement in X-ray activity.

Also the strong X-ray flares of Mrk 421 in 2000/2001 and 2002 were accompanied by strong TeV emission states (Ref. 46, Ref. 2, Ref. 12). Similarly the first strong TeV flaring state detected for 1ES1959+650 in 2002 (Ref. 35) falls together with strong X-ray activity, whereas it was at barely detectable levels in TeV photons before 1999 (Ref. 63). Also in support of the X-ray/TeV connection, is the fact that the blazar 1ES2344+514, was detected in gamma rays (Ref. 15) and showed a weak flux of 0.11 Crab in 1995-1996, and since then has been confirmed by a weak detection by the HEGRA collaboration (Ref. 77), although many attempts for detection were made during 1997-2002. This is consistent with the fact that 1ES2344+514 was in a low emission state in X-rays over the last six years. It is clear from Fig. 5 that these TeV blazars undergo episodes of flaring activity in X-rays that last several days to months. The X-ray/TeV connection has also significantly influenced the search strategy for new TeV blazars, e.g., by conducting surveys of X-ray selected BL Lac objects (Ref. 38, Ref. 19).

In fact the gamma-ray blazars Mrk 501 and H1426+428 (Ref. 37, Ref. 36, Ref. 22, Ref. 3) were discovered by following the paradigm that X-ray and in particularly hard X-ray BL Lac objects (Ref. 18) are prospective TeV gamma-ray emitters. Furthermore,

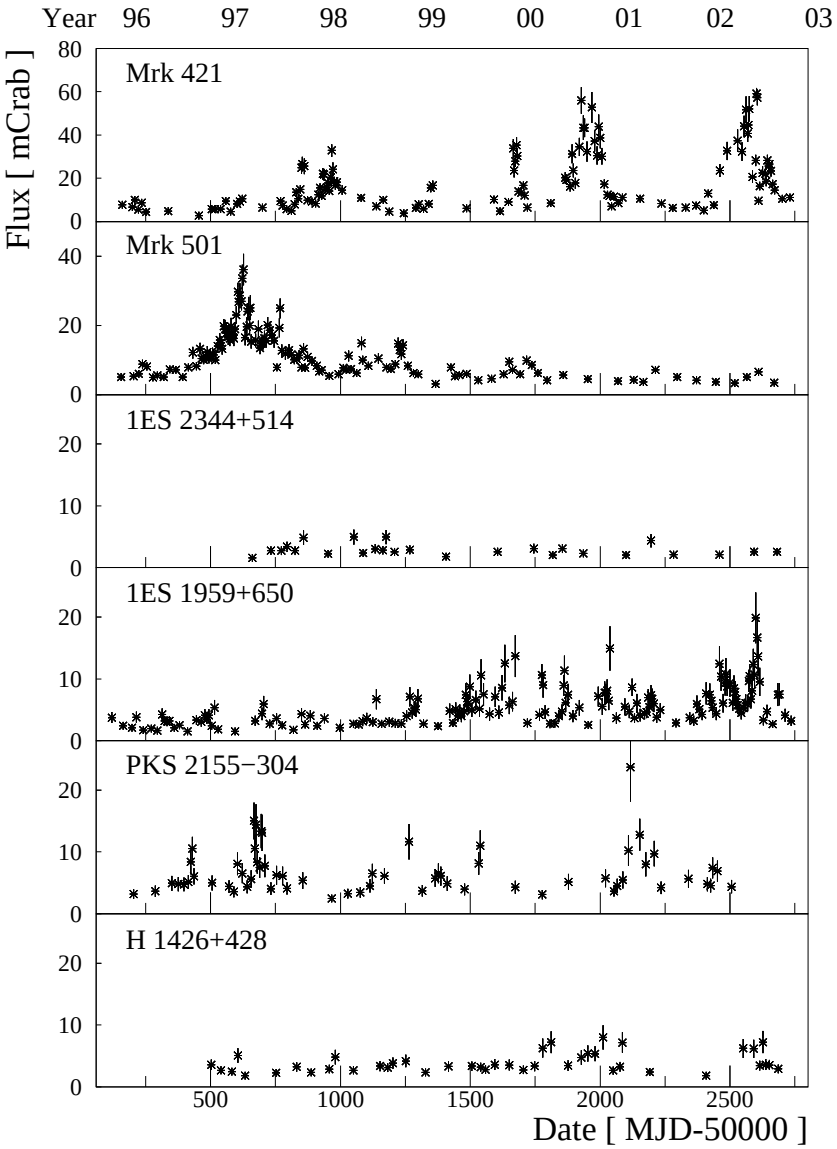

Fig. 5. The lightcurves for the six established TeV blazars at X-rays using the RXTE all-sky monitor. This figure has been adopted from Ref. 44.

these active X-ray episodes provide an alert and the opportunity to study these objects with excellent statistics at VHE gamma-ray energies.

Evidence for daily correlations between VHE gamma-ray emission and X-ray emission for Mrk 421 has been found during various episodes of flaring activity (Ref. 53, Ref. 13 and others) in the mid-1990s. A huge outburst of flaring activity of Mrk 501 in 1997 lasting for half a year provided the opportunity to study the X-ray/gamma ray connection in more detail (see Fig. 5 for X-rays, Fig. 2 for gamma rays and Fig. 6 for both). The correlation between the gamma-ray flux (350 GeV) and the emission state at X-rays (2-25 keV) and hard X-rays (50-150 keV) is illustrated in Fig. 6. The ampli-

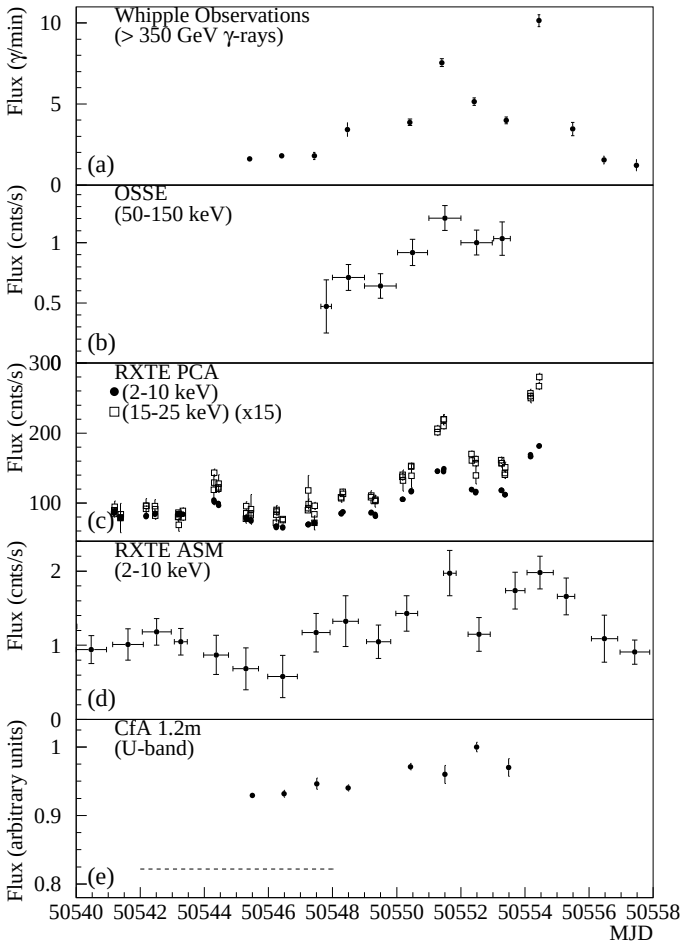

Fig. 6. The lightcurve for Mrk 501 from observations at gamma-ray energies above 400 GeV (top panel), hard X-rays at 50 keV-100 keV (OSSE) and at X-rays (RXTE PCA) at 2 keV-10 keV, at 15 keV-25 keV and complete coverage between 2 keV-10 keV (RXTE ASM). The lowest panel shows the optical lightcurve recorded with the 1.2 m CfA telescopes (Ref. 14).

tude of the flux variation is largest at gamma-ray energies and is progressively smaller at 15 keV-25 keV and 2 keV-10 keV. This is in principle what is expected in an SSC model: the inverse Compton flux depends on the density of the electrons and the energy density of the synchrotron photons which is a direct result from the former. Therefore, a quadratic dependence of the inverse Compton flux from the synchrotron flux would be expected in an SSC model.

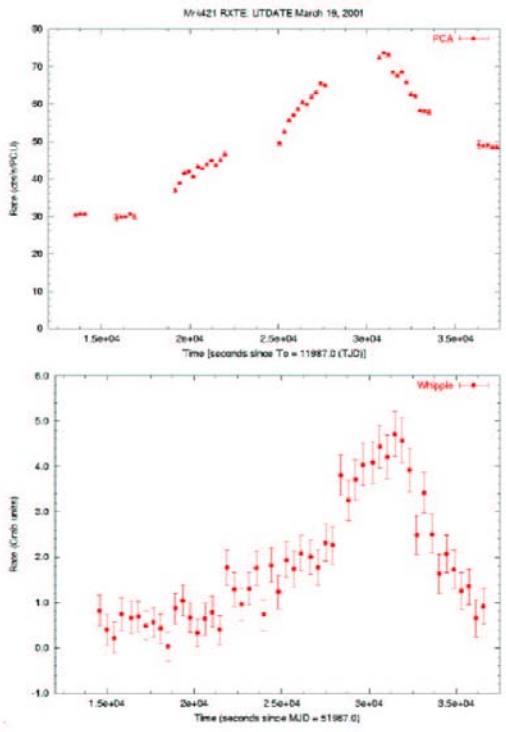

Fig. 7. The lightcurve for Mrk 421 on March 19 2001 measured with the Whipple telescope (Ref. 40).

Motivated by the apparent X-ray/TeV correlation further multiwavelength campaigns were carried out over the following years (Mrk 421 in 1998, 2000, 2001 and 1ES1959+650 in 2002). Particularly interesting are the observations covering a single night for which X-ray and gamma-ray data with almost continuous coverage for a few hours has been achieved. This allows dynamic studies of individual flares and detailed modeling. A well sampled light curve of an individual gamma-ray/X-ray flare of Mrk 421 is shown in Fig. 7: the X-ray flux follows the gamma-ray lightcurve and a correlation is evident to the eye.

A recent study of the gamma-ray/X-ray connection by Krawzcynski et al. (Ref. 44) uses data from the TeV blazar 1ES1959+650 (Ref. 4, Ref. 35). Although this study

suggests an overall correlation between X-ray and TeV photon emission (Fig. 8), these data also show a TeV flare (June 4th 2002) without a corresponding X-ray flux increase. A conclusion from this observation is that this single gamma-ray flare cannot be explained by a one-zone SSC model predicting a contemporaneous X-ray flare. Other emission scenarios have been considered suggesting that the TeV emission comes from a separate region with a second electron population and a soft energy spectrum, or an external Compton model involving the precession of the jet effecting the gamma-ray emission but not the synchrotron photons and proton models, all capable of producing such ”orphan” gamma-ray flares (Ref. 44).

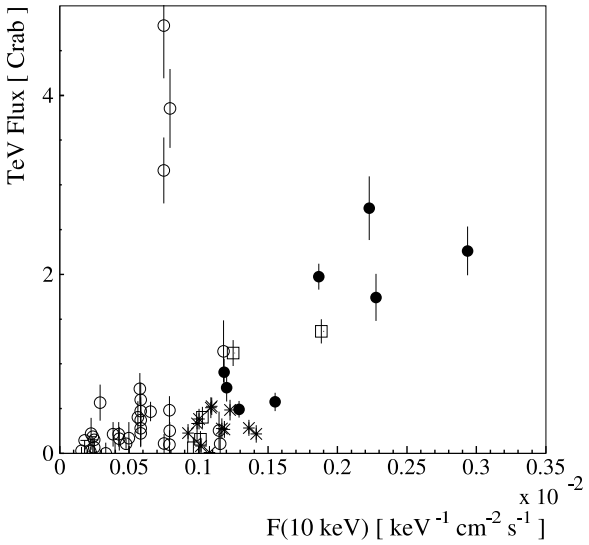

Fig. 8. The correlation between the X-ray flux and gamma-ray fluxes of 1ES1959+650 measured during different epochs in 2002 is shown. The three data points (open circles) to the upper left correspond to a flare on the night of June 4 2002, showing no corresponding flux increase in X-rays (Ref. 44).

Testing blazar emission models requires the measurement of spectra in an energy regime most promising for discriminating various high energy emission models. An example of a clear spectral feature that would be unique to proton models producing gamma rays via neutral pion decay is the 70 MeV bump in low energy gamma rays. Although no comparable smoking gun signature is currently predicted for VHE gamma-ray spectra from blazars, spectral features such as deviations from powerlaws and cutoffs, provide constraints such as the maximum particle energy, cooling time scales and magnetic field strength. The next section is concerned with spectral measurements at TeV energies.

2.3 Spectral Variability of Blazars in Gamma Rays

VHE gamma-ray spectra constitute the high energy end of the electromagnetic spectrum in astronomy. The shape and variations of the spectrum with time are important constraints for emission model parameters such as maximum particle energy, magnetic field strength and Doppler factor. Spectral variability is not unexpected during the rise and the decay of a gamma-ray flare and X-ray flare. For example, in a basic one-zone SSC model a flare could be caused by an increase in the maximum particle energy, leading to a shift of the synchrotron emission peak, translating into spectral variations. As a consequence, the X-ray flux should show a correlation with the X-ray spectral index during a flare. Such a relation has been observed for Mrk 421 during various episodes of X-ray flaring activity (Ref. 23, Ref. 76).

Similarly, spectral variations are expected in the gamma-ray regime assuming they result from inverse Compton scattered synchrotron photons. The strong flares of Mrk 501 in 1997 and Mrk 421 in 2000/2001 provided the opportunity to search for gamma-ray spectral variability. The latter occasion provided more than 20,000 photons above 300 GeV detected with the Whipple 10 m telescope.

Figure 9 a) shows the gamma-ray lightcurve for Mrk 421 on March 19 2001 (Ref. 49), complemented by a measurement of the differential spectral index. The TeV observations provide almost complete sampling of the rise and decay of a flare. The gamma-ray rate ranges from a moderate level ($\approx$ 1 Crab) up to an eight fold flux increase in less than 4.5 hours. The hypothesis that the spectral index is constant during the flare has a chance probability of 3.1×10^{-4}, suggesting spectral variability during this flare with a significance of 3.6σ. When dividing the spectral index measurements into three different episodes, preflare, rising flare and postflare, the hardest spectral index coincides with the rise of the flare, whereas during the preflare and the postflare the spectrum appears to be softer. A similar correlation between hardening/softening of the energy spectrum and flux for Mrk 421 has been reported by the HEGRA collaboration (Ref. **?**) for the nights of March 21/22 and 22/23, 2001.

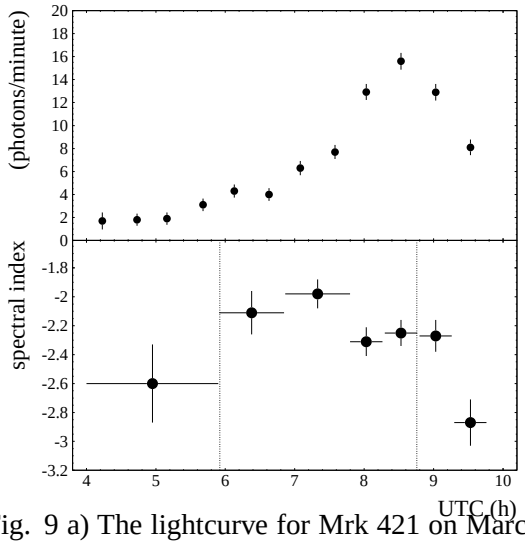

Fig. 9 a) The lightcurve for Mrk 421 on March 19 2001 (top) and the spectral index (below) between 380 GeV-2.6 TeV are shown (Ref. 49).

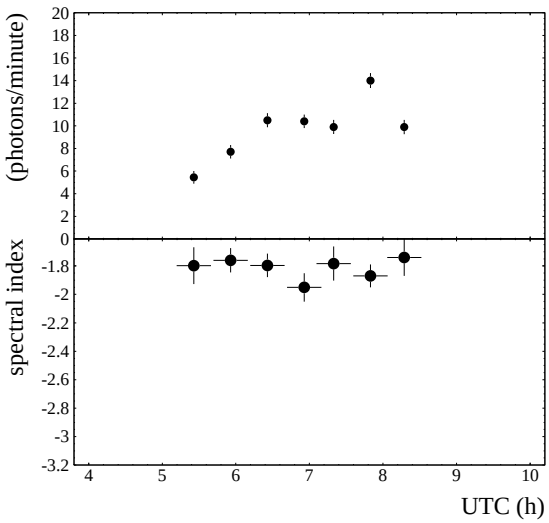

Fig. 9 b) The lightcurve for Mrk 421 on March 25 2001 (top) and the spectral index (below) between 380 GeV-2.6 TeV are shown (Ref. 49).

However, flaring activity during other nights suggest that the relation between spectral index and flux variability is more complex. A flare on March 25 2001 measured with the Whipple 10 m telescope (Fig. 9 b) shows a lightcurve with significant flux variations and a flux increase by a factor of 2.5 within 2 hours. The spectral index during this flare is exceptionally hard ($\alpha = 1.82 \pm 0.04$) without any indications of spectral variability. These data indicate that on time scales of hours the correlation between flux and spectral index is complex, at times showing spectral variability and at other times showing no spectral variation at all. One-zone SSC models that describe gamma-ray flares solely by an increase in the maximum energy of the radiating particle distribution are inconsistent with this observation.

However, when considering longer time scales from several months to years of observations, a different picture unfolds. To study time-averaged spectral variations, the 2000/2001 data of Mrk 421 has been binned by flux, revealing the average luminosity peak energy as it varies with flux.

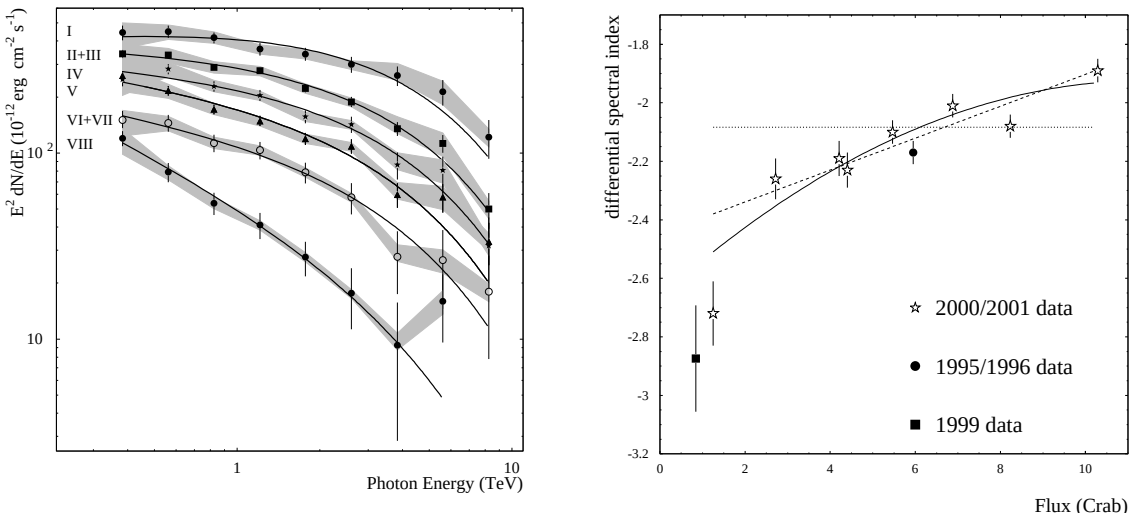

Fig. 10 a) Mrk 421 spectra at different flux levels averaged for data over the 2000/2001 season. The spectra have been fit by a power law with a fixed exponential cutoff at 4.3 TeV (Ref. 47).

Fig. 10 b) The stars show the spectral index of Mrk 421 versus flux in Crab units for the 2000-2001 data, the solid circle and rectangle represents data from 1995/96 and 1999.

Fig. 10 a) exhibits the time averaged energy spectra (2000/2001) of Mrk 421 at different flux levels, showing significantly different spectra as a function of flux. Fig. 10 b) shows the spectral index vs. flux for these data and including archival data from previous observations in 1995/1996 and 1999. A correlation between flux and index is supported by all data points measured over a time period of 6 years. The conclusion is that on average the energy spectrum of Mrk 421 is harder at high flux levels and softer at low flux states, suggesting that the gamma-ray luminosity peak shifts towards higher energies during high emission states. Spectral hardening during flares has also been observed for Mrk 421 in X-rays (Ref. 23, Ref. 76) using BeppoSAX data during X-ray flares in 1997 and 1998. In X-rays, the effect of spectral hardening corresponds to a shift of the synchrotron peak towards higher frequencies.

In order to extract the energy at which the VHE gamma-ray luminosity peaks, it is necessary to consider effects from attenuation by radiation fields in extragalactic space, most importantly for the absorption by the cosmic infrared background. This is the topic of the next section.

2.4 TeV Blazar Spectra and Absorption by the Cosmic Infrared Background

Whereas the universe is transparent to gamma rays below 10 GeV, extragalactic diffuse radiation fields become an obstacle to TeV photons traveling over distances of a few 100 Mpc or more. In fact our view of the universe beyond our own galaxy in 100 TeV photons is essentially obscured by pair-production of gamma rays with photons of the cosmic microwave background (CMB). Although the CMB is a great obstacle to gamma-ray astronomy above 100 TeV, the interaction of sub-TeV to multi-TeV photons with extragalactic diffuse radiation has been recognized (Ref. 27, Ref. 75) as an opportunity to make a potentially important contribution to cosmology, by constraining the extragalactic background light (EBL). The EBL is part of the diffuse extragalactic background radiation spectrum that ranges from 10^{-7} eV (radio background) to almost 10^{11} eV (gamma-ray background). Although the diffuse radiation is dominated by the CMB, the EBL is the second most dominant form of electromagnetic energy density throughout the universe. The EBL originates from the time of structure/galaxy formation and evolution (Ref. 66, Ref. 68) and contains important cosmological information about how galaxies formed. Direct measurements of the EBL in the mid-infrared are extremely difficult due to the presence of strong foreground zodiacal emission consisting of scattered light and thermal emission from interplanetary dust particles (Ref. 41). For an extensive review, see the paper by Hauser & Dwek (Ref. 32).

It is therefore generally believed that energy spectra of gamma-ray blazars between sub-100 GeV and multi-TeV energies contain an imprint from the EBL due to gamma-ray pair-production (Ref. 27, Ref. 75) with soft photons in the near-infrared to mid-infrared. The signature of this imprint depends on the spectral shape of the EBL, making TeV gamma-ray spectra strong constraints to the EBL density in the wavelength regime of 0.1 μm - 30 μm.

For the discussion of TeV blazar spectra in the context of emission models and multiwavelength studies, a correction for gamma-ray absorption effects by the EBL is required. The difficulty to date is that only a few sources have been detected and statistical studies using a large number of sources are not available. Different attempts have been made to correct blazar spectra for EBL absorption. EBL scenarios based on theoretical models of galaxy formation and evolution (Ref. 68) have been used to correct TeV gamma-ray spectra for EBL absorption. Others have developed semi-empirical scenarios to construct a tentative EBL spectrum (Ref. 54, Ref. 42) for correcting blazar

spectra.

An alternative approach to extract the intrinsic blazar spectra has been taken by Dwek and Krennrich (Ref. 20, Ref. 49), using a range EBL realizations consistent with EBL data comprised of constraints from upper and lower limits and few direct measurements. The latter method explores the entire range of possible EBL scenarios, leading to a large range for the absolute luminosity of the corrected gamma-ray spectra. However, a dip in the EBL density between 1 μm and about 10 μm originating from the stellar and dust emission peak, causes a decrease in the rise of the gamma-ray opacity between 1 and 5 TeV. This dip is common to all EBL scenarios and is beneficial for constraining the intrinsic spectrum of nearby blazars.

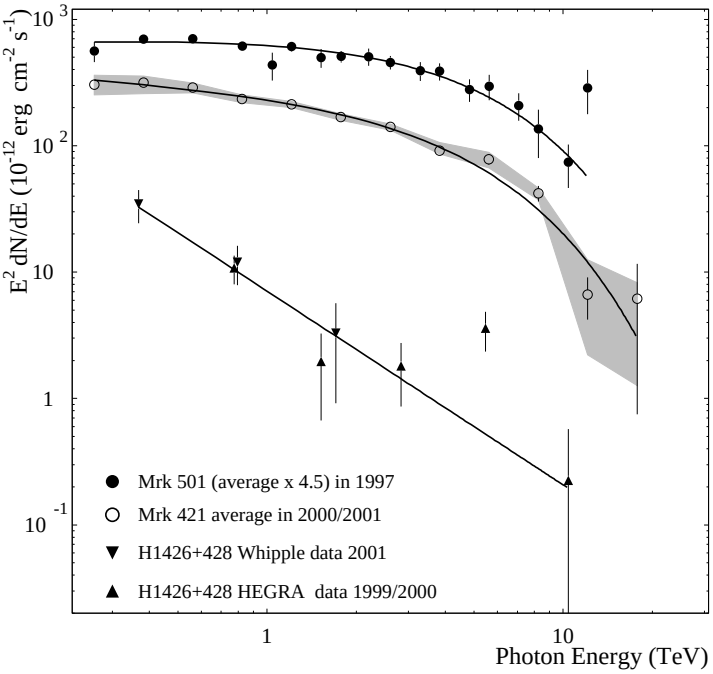

Fig. 11. The average energy spectrum of Mrk 501 (filled circles) in 1997 (Ref. 74) is shown in comparison to the average spectrum of Mrk 421 (empty circles) in 2000/2001 (Ref. 46). Furthermore, a combined energy spectrum of H1426+428 using data from the HEGRA (Ref. **?**) and Whipple collaboration (Ref. 67) is shown.

The two most prominent blazars Mrk 421 and Mrk 501 are nearby and have approximately the same redshift (z=0.031, 0.034 respectively) and therefore any absorption feature in their spectra should be common to both. The energy spectra of Mrk 421, Mrk 501 and H1426+428 are presented in Fig. 11. Both Mrk 421 and Mrk 501 show

a cutoff at approximately 4 -6 TeV as measured by different groups (Ref. 74, Ref. 46, Ref. 2, Ref. 1, Ref. 21). Systematic uncertainties in the absolute energy calibration of the different Cherenkov experiments may be as large as 25%, allowing uncertainties in the cutoff energies at a similar level. The Whipple energy spectra of Mrk 421 and Mrk 501 show both a cutoff energy of approximately 4 TeV. The blazar H1426+428 on the other hand is at a redshift of z=0.129 and its spectrum should be strongly absorbed regardless of the EBL scenario considered. H1426+428 shows a very steep spectrum (Fig. 11) which could be due to strong EBL attenuation.

Figure 12 shows the range of absorption corrected average energy spectra of Mrk 421 and Mrk 501 using the HEGRA data (Whipple data show very similar corrected spectra) based on a correction exploring the entire range of EBL realizations given by Dwek & Krennrich (Ref. 20). The peak energies for Mrk 421 range between 0.5-1.2 TeV and for Mrk 501 between 0.8-2.5 TeV. It is clear from figure 12 that gamma-ray spectra of the nearby blazars are already strongly absorbed at energies above 0.5 TeV. Furthermore, when considering the EBL scenarios consistent with experimental constraints in the infrared, the blaxars seem to peak at similar energies between 0.5 - 2.5 TeV.

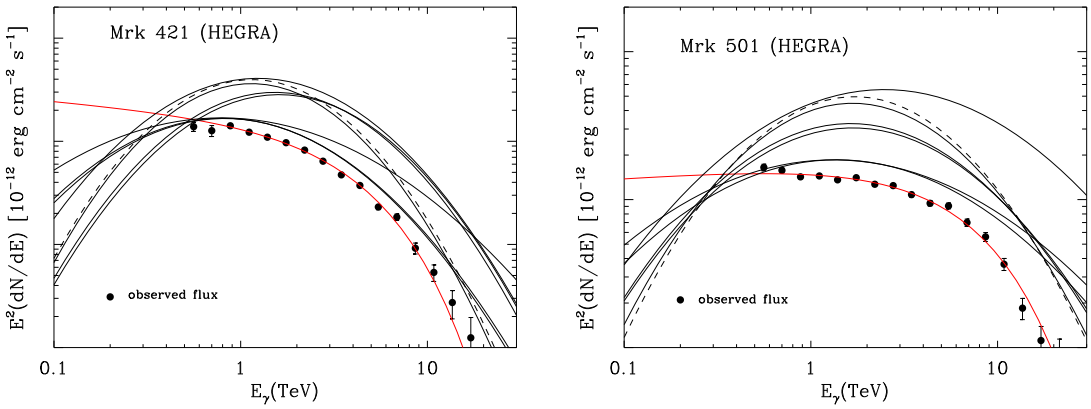

Fig. 12 a) The Mrk 421 spectrum is shown (solid circles) including a parabolic fit. Also the absorption corrected spectral fits for various allowed EBL scenarios are presented (Ref. 20).

Fig. 12 b) The Mrk 501 spectrum is shown (solid circles) including a parabolic fit. Also the absorption corrected spectral fits for various allowed EBL scenarios are presented (Ref. 20).

3 M87: TeV Gamma Rays from Radio Galaxies

Most of the AGN detected at TeV energies are blazars; however, two reports of weak detections suggest that nearby radio galaxies may be emitting TeV photons. Cen A was detected with a first generation atmospheric Cherenkov telescope (Ref. 28) at the 4 sigma level about 28 years ago. Recently, the HEGRA collaboration reported (Ref. 5) the detection of M 87, a nearby ($\mathrm{D} \simeq 16\mathrm{Mpc}$) giant elliptical radio galaxy (Virgo-A).

Due to their proximity both M87 and Cen A allow detailed studies of their relativistic jets in the radio, optical and X-ray regime partially resolving the jet structure, providing a unique perspective for studies of AGN jets which is not accessible for distant blazars. M87 received further attention recently, when it was considered to be the source for most Ultra High Energy cosmic rays (Ref. 10). VHE gamma ray studies currently provide highest energy insights into jets and could potentially provide important clues about the highest energies particles present in M87.

M87 is also known as a Fanaroff-Riley Class I (FR-I) object, referring to its one sided jet that is mis-aligned by about 30° (Ref. 9) from the observer's line of sight. The jet emission extends from the radio, optical (Ref. 59) into the X-ray regime, all exhibiting structure in the jet. The similar morphology of the jet in the radio, optical and X-rays suggest that these have a common origin. Polarization measurements in the optical (Ref. 7, Ref. 24, Ref. 65) and spectral information at X-ray and radio energies (Ref. 73, Ref. 29, Ref. 11) suggest synchrotron emission as the mechanism. Variability measurements at X-rays (Ref. 30) and electron cooling time scales suggest the presence of 10 TeV electrons (Ref. 29), providing a key condition for inverse Compton scattering of soft photons to TeV gamma-rays (Ref. 11) in the jet. Hence, gamma-ray emission would be expected in the framework of SSC models; however, large uncertainties in the flux prediction leave ample room for other scenarios.

A possibility involving large magnetic field strengths in the jet for the region of TeV photon production is described by the Synchrotron Proton Blazar (SPB) model, providing a possible link to the origin of Ultra High Energy Cosmic Rays cosmic rays (Ref. 10). Other possibilities of TeV gamma-ray emission involve the annihilation of super-symmetric particles (Ref. 8) from a dark matter halo and a larger scale for M87.

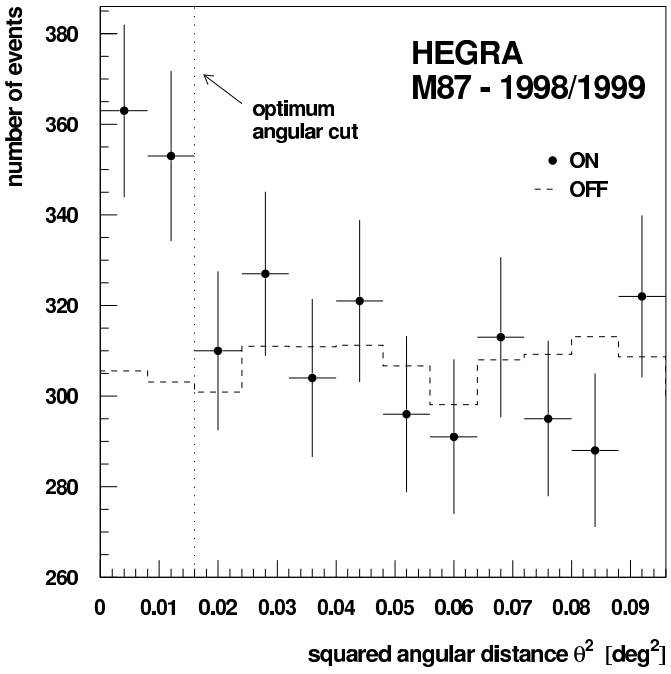

Fig. 13. The angular distribution for the ON-source observations and the background data for M87. From Ref. 5.

Observations of M87 have been pursued by the HEGRA and Whipple collaboration and both groups initially reported upper limits (Ref. 26, Ref. 50). The HEGRA collaboration, after applying a more sensitive analysis method, recently reported a 4σ detection based on 83.4 hours of observation with a flux of approximately 3.3% of the Crab flux above $730\ \mathrm{GeV}$ (Ref. 5). Although statistically marginal, this result shows a convincing angular distribution for the arrival direction of the excess events (Fig. 13). Observations by the Whipple collaboration (Ref. 51) report an upper limit of 8% of the Crab flux at 400 GeV providing together with the HEGRA detection additional spectral constraints. Future observations of M87 with next generation atmospheric Cherenkov telescopes will be focused on variability studies together with correlated observations at X-rays to distinguish between an SSC model and the other possible TeV photon emission scenarios.

Although interesting the detection of the radio galaxies Cen A and M87 at VHE energies requires confirmation.

4 The First TeV Unidentified Source

Atmospheric Cherenkov telescopes have a narrow field of view and are operated at a 10% duty cycle; hence, to date only about 5% of the sky has been observed at 0.5 TeV with a sensitivity of 0.1 Crab. However, a serendipituous discovery of a TeV source (TEV2032+4130) was made by the HEGRA collaboration (Ref. 3) when observing Cygnus-X3 and the EGRET source GeV J2035+4214 in the Cygnus region.

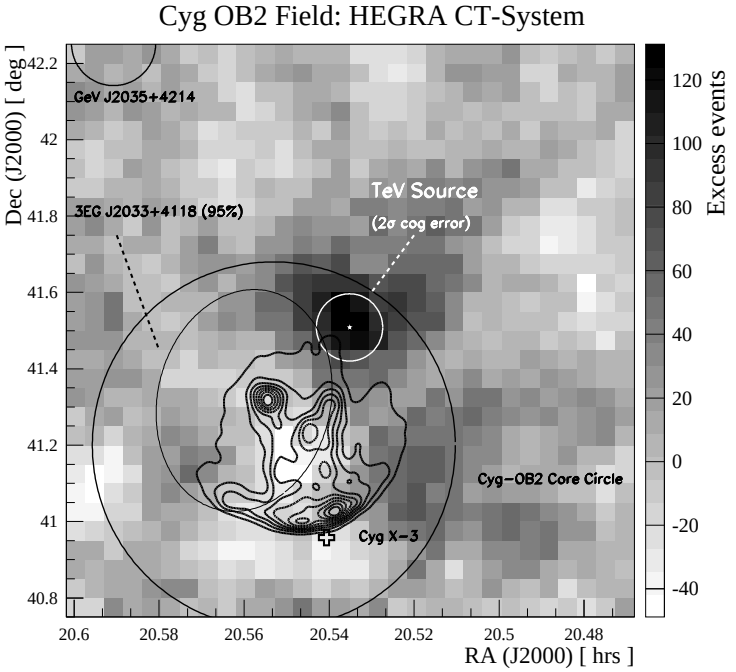

Fig. 14. The skymap of excess events around the new TeV source TEV2032+4130 also showing Cygnus X-3 and two EGRET sources. Also shown is the OB association Cygnus OB2 (Ref. 3).

The source was initially detected at the 4.6 sigma level based on 113 hours of data and was recently confirmed by the HEGRA collaboration using new observations from 2002 (presented at the 28th ICRC, Tsukuba). TEV2032+4130 has a differential spectral index of $\alpha = 1.9 \pm 0.3$, which is a hard spectrum. Hence, the spectrum indicates that the luminosity peak in gamma rays may be in the TeV regime. Given the superb angular resolution of imaging atmospheric Cherenkov telescope arrays, the HEGRA collaboration was also able to constrain the source size, indicating at the 3 sigma level, that it is an extended object ($5.6' \pm 1.7'$) rather than a point source.

The origin of the TeV source is unclear, no unambiguous identification with an as-

trophysical counterpart has been made. However, the TeV emission could be associated with the OB association Cygnus OB2 containing a large number of OB and O stars. Particle acceleration in OB associations has been considered in earlier theoretical studies (Ref. 61, Ref. 79). To understand the origin of the TeV radiation X-ray studies will be critical to assess whether the TeV gamma rays are produced by inverse Compton scattering of soft photon fields or arise from a hadronic origin.

5 The Future

Most observations discussed in this review were obtained with second generation imaging atmospheric Cherenkov telescopes, involving the Whipple observatory 10 m gamma-ray telescope, the HEGRA array of five 4 m diameter telescopes and the CAT 5 m diameter telescope. All three instruments have in common that they were able to detect the Crab Nebula at a statistical significance of more than 5 sigma in one hour time, making them all roughly equally sensitive with some differences in their low and high energy response, background rejection and energy resolution.

Next generation atmospheric Cherenkov telescopes are all based on the imaging technique pioneered by the Whipple collaboration and using the stereoscopic technique implemented successfully by the HEGRA collaboration. A combination of large diameter telescopes, improved electronics, better optics and high rate data acquisition systems are the basis of the next generation instruments such as MAGIC (Ref. 52), HESS (Ref. 34) and VERITAS (Ref. 82) and CANGAROO-III (Ref. 64). These instruments will reach about an order of magnitude more sensitivity than the previous generation telescopes. This will allow the study of the TeV sources with 5 mCrab sensitivity (50 hours, 5 sigma detection), making even the weakest sources reported above strong detections.

Furthermore, the next generation telescopes will have an energy threshold in the sub-100 GeV regime. This is the energy regime for which the opacity of the universe due to the diffuse extragalactic background light is greatly reduced and these ground-based gamma-ray telescopes will be able see out to redshifts of z=1. The greatly increased gamma-ray horizon of the universe will allow the study of ten's of blazars or more and provide important constraints on the diffuse near-infrared to far-infrared light.

6 Acknowledgements

This research is supported by the U.S. Department of Energy. I thank David Carter-Lewis, Stephan LeBohec and Trevor Weekes for comments on the paper.

References

[1] F.A., Aharonian et al., A& A, 349, 11 (1999).

[2] F.A., Aharonian et al., A& A, 384, 834 (2002a).

[3] F.A., Aharonian et al., A& A, 393, L37 (2002b).

[4] F.A., Aharonian et al., A& A, 406, L9 (2003a).

[5] F.A., Aharonian et al., A& A, 403, L1 (2003b).

[6] J.R.P. Angel & H.S. Stockman, ARAA, 18, 321 (1980).

[7] W. Baade, ApJ, 123, 550 (1956).

[8] E.A. Baltz, et al., Phys. Rev. D61 023514 (2000).

[9] G.V. Bicknell & M.C. Begelman, ApJ, 467, 597 (1996).

[10] P.L. Biermann et al. 2001, Lecture Notes in Physics, 576, 181 (2001).

[11] J.A. Biretta, AJ, 101, 1632 (1991).

[12] L.M. Boone et al., ApJ, 579, L5 (2002).

[13] J.H. Buckley, ApJ, 472, L9 (1996).

[14] M. Catanese, ApJ, 487, L143 (1997).

[15] M. Catanese, ApJ, 501, 616 (1998).

[16] M. Catanese & T.C. Weekes, PASP, 111, 1193 (1999).

[17] P. Coppi, Proc. of “The Universe Viewed in Gamma Rays”, University of Tokyo Symp., eds. R. Enomoto, M. Mori, S. Yanagita (Kashiwa, Japan), p.77 (2002).

[18] L. Costamante & G. Ghisellini, A&A, 384, 56 (2002).

[19] I. De la Calle Perez et al., ApJ, 599, 909 (2003).

[20] E. Dwek & F. Krennrich, in preparation, (2004).

[21] A. Djannati-Atai et al., A&A , 350, 17 (1999).

[22] A. Djannati-Atai et al., A&A , 391, L25 (2002).

[23] G. Fossati et al., ApJ, 541, 166 (2000).

[24] D. Fraix-Burnet et al., A&A, 224, 17 (1989).

[25] J.A. Gaidos et al., Nature, 383, 319 (1996).

[26] N. Götting et al., in Proc. of the 27th ICRC (Hamburg), OG 2.3, 199 (2001).

[27] R. J. Gould & G. Schréder, Phys. Rev., 155, 1408 (1967).

[28] J.E. Grindlay et al., ApJ, 197, L9 (1975).

[29] D.E. Harris & H. Krawczynski, ApJ, 565, 244 (2002)

[30] D.E. Harris et al., ApJ, 586, L41-L44 (2003).

[31] R.C. Hartman et al., ApJS, 123, 79 (1999).

[32] M.G. Hauser & E. Dwek, ARA&A, 39, 249 (2001).

[33] S.W. Hawking, Nature, 248, 31 (1974).

[34] W. Hofmann et al., Proc. of "The Universe Viewed in Gamma Rays", University of Tokyo Symp., eds. R. Enomoto, M. Mori, S. Yanagita (Kashiwa, Japan), p.357 (2002).

[35] J. Holder et al., ApJ, 583, L9 (2002).

[36] D. Horan et al., HEAD meeting, Hawaii, No. 23, 05.03 (2000).

[37] D. Horan et al., ApJ, 571, 753 (2002).

[38] D. Horan et al., ApJ, in press (see also astro-ph0311397) (2003).

[39] D. Horan & T.C. Weekes, New Astronomy Reviews, Summary talk at "2nd VERITAS Symposium of TeV Astrophysics of Extragalactic Sources", in press (2003).

[40] M. Jordan et al., Proc. of the 27th ICRC (Hamburg), 2691 (2001).

[41] T. Kelsall et al., ApJ, 508, 44 (1998).

[42] T. Kneiske & K. Mannheim, A & A, in press (2003)

[43] A. Konopelko et al., April APS/HEAD Meeting, Albuquerque, Session B17 (2002).

[44] H. Krawzcynski et al., ApJ, in press (2003).

[45] F. Krennrich et al., ApJ, 511, 149 (1999).

[46] F. Krennrich et al., ApJ, 560, L45 (2001).

[47] F. Krennrich et al., ApJ, 575, L9 (2002).

[48] F. Krennrich et al., Proc. of the 28th ICRC, OG2.3, 2603 (2003).

[49] F. Krennrich & E. Dwek, Proc. of the 28th ICRC, OG2.3, 2667 (2003).

[50] S. LeBohec et al., Proc. of the 27th ICRC (Hamburg), OG 2.3, 191 (2001).

[51] S. LeBohec et al., submitted to ApJ (2003).

[52] E. Lorenz et al., Proc. of "The Universe Viewed in Gamma Rays", University of Tokyo Symp., eds. R. Enomoto, M. Mori, S. Yanagita (Kashiwa, Japan), p.351 (2002).

[53] D. Macomb et al., ApJ, 449, L99 (1995).

[54] M.A. Malkan & F.W. Stecker, ApJ, 555, 641 (2001).

[55] K. Mannheim, & P.L. Biermann, A&A, 253, L21 (1992).

[56] K. Mannheim, A&A, 269, 67 (1993).

[57] K. Mannheim, Science, 279, 684 (1998).

[58] L. Maraschi, G. Ghisellini, & A. Celotti, ApJ, 397, L5 (1992).

[59] H.L. Marshall et al., ApJ, 564, 683 (2001).

[60] A.P. Marscher, & J.P. Travis, A&AS, 120, 537 (1996).

[61] T. Montmerle, ApJ, 231, 95 (1976).

[62] A. Mücke & R.J. Protheroe, Astropart. Phys., 15, 121 (2001).

[63] T. Nishiyama et al., Proc. 26th ICRC, Vol. 3, 370 (1999).

[64] M. Ohishi et al., Proc. of "The Universe Viewed in Gamma Rays", University of Tokyo Symp., eds. R. Enomoto, M. Mori, S. Yanagita (Kashiwa, Japan), p.363 (2002).

[65] F.N. Owen, et al. ApJ, 340, 698 (1989).

[66] R.B. Partridge & P.J.E. Peebles, ApJ, 148, 377 (1967).

[67] D. Petry et al., ApJ, 580, 104 (2002).

[68] J.R. Primack, Astropart. Phys., 11, 93 (1999).

[69] R. Protheroe et al., Proc. 25th ICRC (Durban), 8, 317 (1997).

[70] M. Punch et al. 1992, Nature, 358, 477 (1992).

[71] L. Bergström and J. Kaplan, Astropart. Phys. 2, 261 (1994).

[72] J. Quinn et al., ApJ, 518, 693 (1999).

[73] S. Reynolds et al., ApJ, 521, 99 (1999).

[74] F.W. Samuelson et al., ApJ, 501, L17 (1998).

[75] F.W. Stecker, O.C. de Jager, & M.H. Salamon, ApJ, 390, L49 (1992).

[76] C. Tanihata et al., ApJ, in press (2004).

[77] M. Tluczykont et al., Proc. of the 28th International Cosmic Ray Conference (Tsukuba, Japan), 2547 (2003).

[78] P. Ullio and L. Bergström, Phys. Rev. D 57, 1962 (1998); Z. Bern, P. Gondolo, and M. Perelstein, Phys. Lett. B 411, 86 (1997).

[79] H.J. Voelk & M. Forman, ApJ, 253, 188 (1982).

[80] T.C. Weekes et al., ApJ, 342, 379 (1989).

[81] T.C. Weekes et al., Astropart. Phys., 17, 221 (2002).

[82] T.C. Weekes, Plenary talk at the 28th International Cosmic Ray Conference (Tsukuba, Japan), in press (2003).